REFERENCES

[1] S. B. Cohn, "Slot line on a dielectric substrate," *IEEE Trans. Microwave Theory Tech.*, vol. MTT-17, pp. 768–778, Oct 1969.

[2] E. A. Mariani *et al*, "Slot line characteristics," *IEEE Trans. Microwave Theory Tech.*, vol. MTT-17, pp. 1091–1096, Dec. 1969.

[3] T. Itoh and R. Mittra, "Dispersion characteristics of slot lines," *Electron. Lett*, vol. 7, pp. 364–365, July 1971.

[4] J. B. Knorr and K. Kuchler, "Analysis of coupled slots and coplanar strips on dielectric substrate," *IEEE Trans. Microwave Theory Tech.*, vol. MTT-23, pp. 541–548, July 1975.

[5] R. Garg and K. C. Gupta, "Expressions for wavelength and impedance of a slot line," *IEEE Trans. Microwave Theory Tech.*, vol. MTT-24, pp. 532, Aug. 1976.

[6] J. B. Davies and D. Mirshekar-Syahkal, "Spectral domain solution of arbitrary coplanar transmission line with multilayer substrate," *IEEE Trans. Microwave Theory Tech.*, vol. MTT-25, pp. 143–146, Feb. 1977.

[7] E. L. Kollberg *et al.*, "New results on tapered slot endfire antennas on dielectric substrate," presented at 8th IEEE Int. Conf. on Infrared and millimeter waves, Miami, Dec. 1983.

[8] K. S. Yngvesson, "Near-millimeter imaging with integrated planar receptors: General requirements and constraints," in *Infrared and Millimeter Waves*, vol 10, K. J. Button. Ed. New York: Academic Press.

[9] S. N. Prasad and S. Mahapatra, "A new mic slot-line aerial," *IEEE Trans. Antennas Propagat*, vol AP-31, no. 3, pp. 525–527, May 1983.

[10] T. Itoh, "Spectral domain immitance approach for dispersion characteristics of generalized printed transmission lines," *IEEE Trans. Microwave Theory Tech.*, vol. MTT-28, pp. 733–736, July 1980.

[11] A. Erdelyi, *Tables of Integral Transforms*, vol. 2. New York: McGraw-Hill, 1954.

Transient Analysis of Microstrip Gap in Three-Dimensional Space

SHOICHI KOIKE, NORINOBU YOSHIDA, AND ICHIRO FUKAI

Abstract — **In this paper, we deal with the microstrip gap that should be analyzed in three-dimensional space. The time variations of the electric field at each surface of the stripline having a finite metallization thickness are analyzed. Our method of analysis is based on both an equivalent circuit of Maxwell's equations and Bergeron's method. The former has advantages in the vector analysis by using all electromagnetic components. The latter has advantages in the time-domain analysis of the field. Therefore, our method can analyze field variations in three-dimensional space and time. We present the time variation of the instantaneous electric-field distributions below the strip, at the side of the strip, and at the gap end surface. These results show how the steady-state field distribution grows in the gap.**

I. INTRODUCTION

The microstrip gap is important as a coupling component in MIC [1], [2]. In this paper, we analyze the microstrip gap in three-dimensional space [3]. The transient analysis of the electromagnetic field is not only useful in clarifying the field response but also yields information on the mechanism by which the distribution of the electromagnetic field in the stationary state is brought about. We have recently proposed a new numerical method for the transient analysis of the electromagnetic field in three-dimensional space by formulating the equivalent circuit which simulates Maxwell's equations by Bergeron's method [4], [5]. We analyze the microstrip gap with this method, taking into account the thickness of the strip conductor. This paper presents the time variation of the instantaneous electric-field distributions below the strip, at the side of the strip, and at the gap end surface. These results show how the steady-state field distribution grows in the gap.

Manuscript received November 27, 1984; revised March 18, 1985.

The authors are with the Faculty of Engineering, Hokkaido University, Sapporo, 060 Japan.

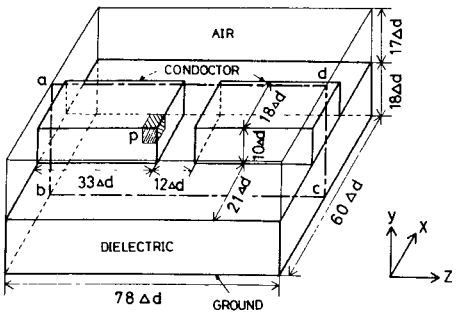

Fig. 1. Model of microstrip gap.

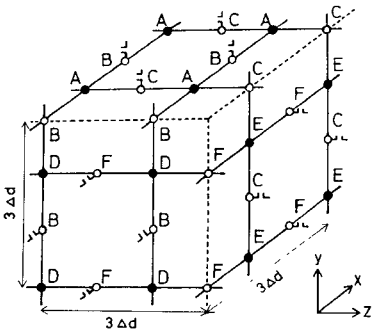

Fig. 2. Arrangement of nodes on the surfaces of the conductor.

II. ANALYZED MODEL OF THE MICROSTRIP GAP

In Fig. 1, the model of the microstrip gap is shown. In this figure, Δd is the interval between adjacent nodes in the equivalent circuit, and the plane *abcd* is a plane of symmetry with respect to the x-direction. In order to model this structure by Bergeron's method, three principal conditions are introduced, namely the boundary condition at the strip conductor, the boundary condition at the free boundary which is the surface of the analyzed region, and the condition of the dielectric. In this paper, we do not give the details of these formulations. But the boundary condition at the conductor is explained in detail because it is important in the formulation. In this analysis, the conductor is supposed to have infinite conductivity, so the tangential components of the electric field and the normal components of the magnetic field on the surface of the conductor should be zero. For example, the equivalent circuit of the part designated by p on the strip conductor in Fig. 1 is presented in Fig. 2. In this figure, the notations ●, ○, and ⊣ represent the electric node in which the voltage variable corresponds to the electric-field component, the magnetic node in which the voltage variable corresponds to the magnetic-field component, and the open-circuit condition, respectively. So the equivalent circuit for the surface of the conductor is realized by: 1) short-circuiting the node on the surface, in which the tangential component of the electric field or the normal component of the magnetic field corresponds to the voltage variable; 2) open-circuiting the node, in which the preceding electromagnetic component corresponds to a current variable. Fig. 2 shows the resultant equivalent circuit obtained by the above-mentioned treatment of the boundary

0018-9480/85/0800-0726$01.00 ©1985 IEEE

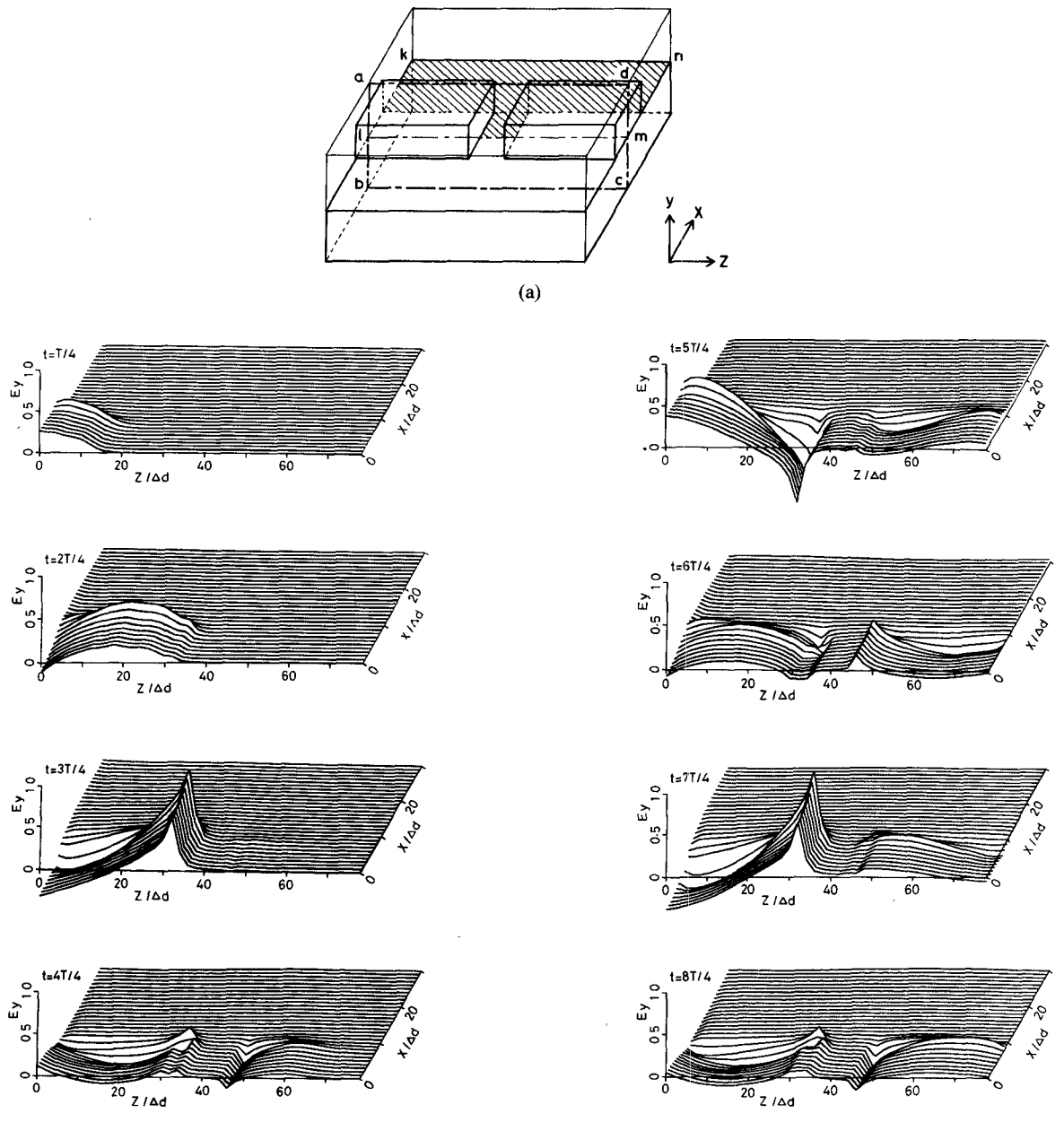

Fig. 3. Transient response of the electric field E_y in the $x-z$ plane below the upper conductor. (a) Observation plane of the electric field E_y. (b) Configuration of the electric field E_y at each time step.

condition for the strip conductor. The details of the correspondence between the equivalent-circuit variables and the electromagnetic variables are shown in [5, table I]. For example, at the B or C nodes on the surface, the branch in the y-direction is open-circuited because the current in the y-direction corresponds to the tangential component of the electric field, namely E_x or E_z, which are both equal to zero. But at the A nodes, the connection to the adjacent nodes is established as usual because the voltage variable which corresponds to the electric field E_y, and each current variable which corresponds to the magnetic-field component H_x or H_z, respectively, exists on the surface. The equivalent circuit of any nodes on other surfaces of the conductor is established in the same manner. The nodes situated on the edge shown by the broken line in Fig. 2 are interconnected according to the diffraction phenomena affecting the incident wave. In this analysis, these nodes have connections to both adjacent planes because the wave propagates along both directions. For example, the B node is positioned at the edge formed by the upper plane and the side plane of the conductor, so both the connections to the A nodes in the x-direction on the upper plane and to the D nodes in the y-direction on the side plane exist. The formulation of the boundary condition at the C and F nodes on other edges of the conductor is realized in the same manner.

III. Results and Discussion

In the analyzed model of the microstrip gap shown in Fig. 1, all dimensions are normalized to Δd. These quantities are also expressed as fractions of λ_g as follows. The thickness of the

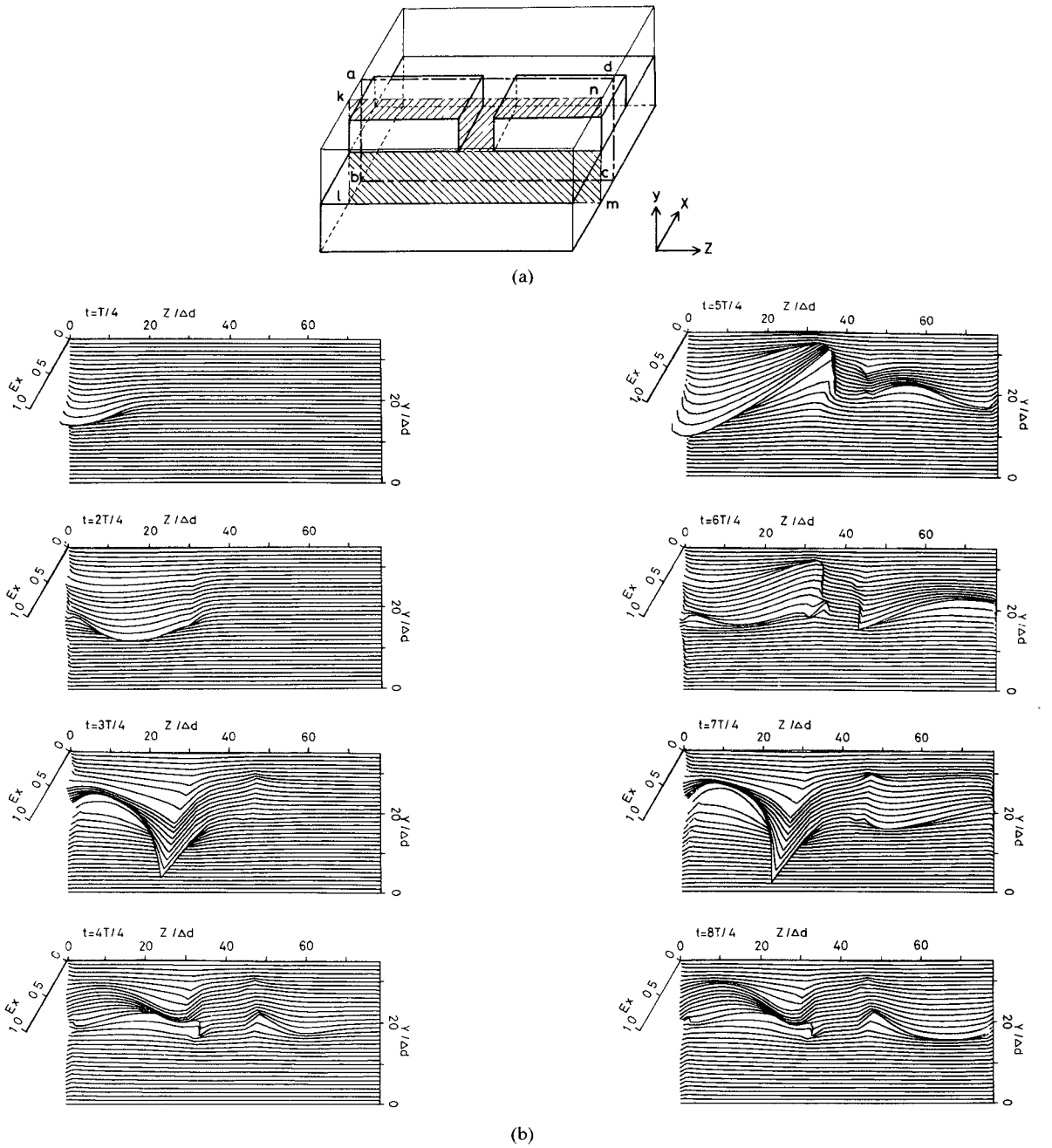

Fig. 4. Transient response of the electric field E_x in the $y-z$ plane beside the conductor. (a) Observation plane of the electric field E_x. (b) Configuration of the electric field E_x at each time step.

dielectric $H = 0.26\ \lambda_g$, the width of the strip conductor $W = 0.26\ \lambda_g$, the gap length $G = 0.17\ \lambda_g$, and the thickness of the strip conductor $D = 0.15\ \lambda_g$. The period T of the sinusoidal incident wave is 426 Δt, where Δt is the time interval between iterations and corresponds to the propagation time between the adjacent nodes in the equivalent circuit. This period is sufficient for good resolution in the time domain.

In Figs. 3–6, the obtained instantaneous field distribution is shown in the plane *klmn* as defined in the *a*-part of each figure. Instantaneous values of the electric field are observed at intervals of $T/4$ from $t = 0$ to $t = 2T$. The initial time $t = 0$ corresponds to the incidence of the wave at $z = 0$. At this time, all components of the electromagnetic field are assumed to be zero. The relative permitivity of the dielectric is 9.6.

Fig. 3(b) shows the transient response of the electric field E_y in the *klmn* plane defined by Fig. 3(a). The field is symmetrical about the $z-y$ plane, so only one half of the field distribution is shown. In Fig. 3(a), the hatched part corresponds to the interface between dielectric and air, and the nonhatched parts correspond to the interface between dielectric and conductor. Fig. 3(b) shows successive stages of the transient wave, and each figure can be interpreted as follows. At $t = T/4$, the wave has not yet reached the gap. At $t = 2T/4$, the field begins to rise at the gap, but the distinct change of the wave form due to the concentration of the

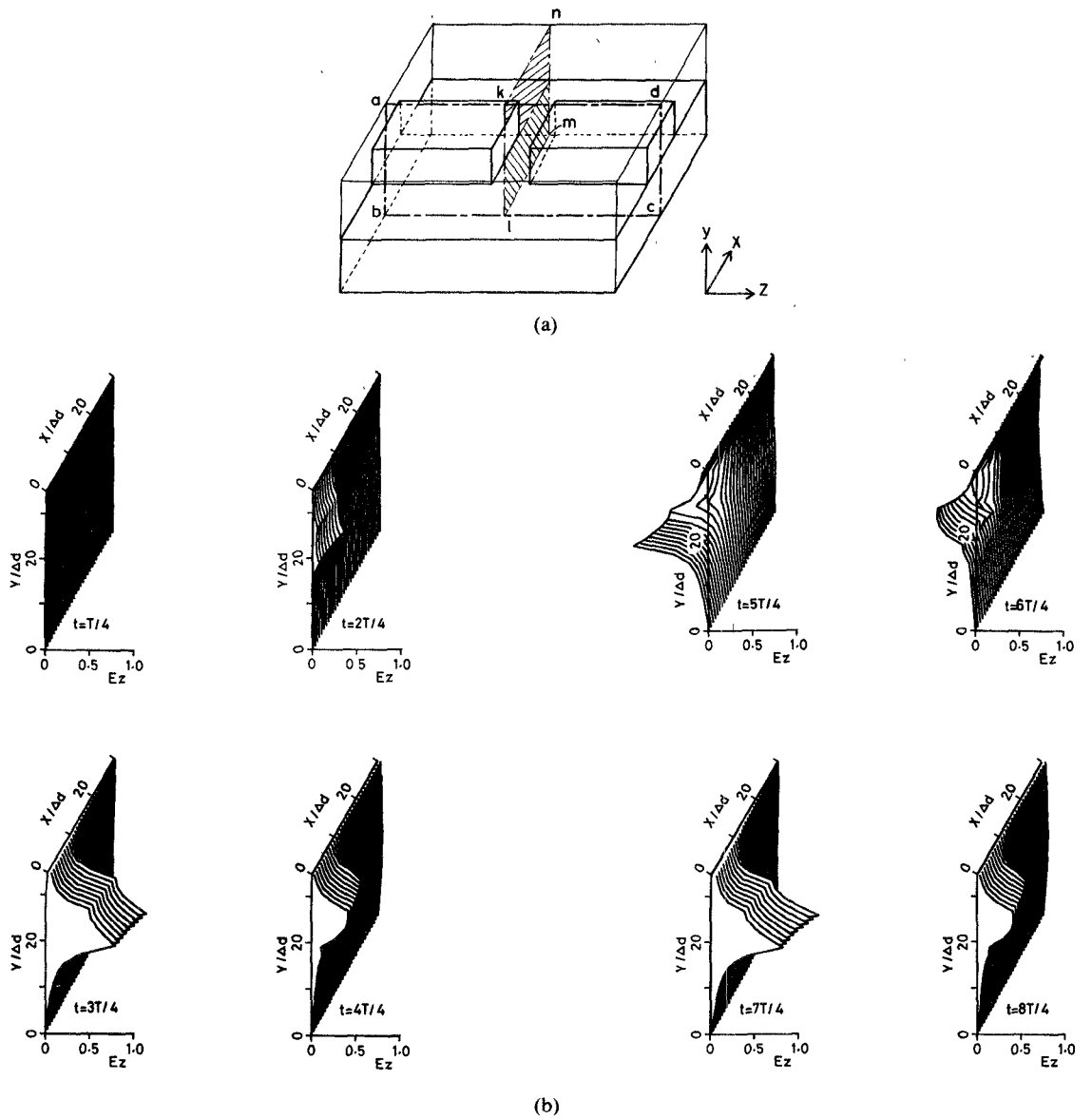

Fig. 5. Transient response of the electric field E_z in the input side plane of the gap. (a) Observation plane of the electric field E_z. (b) Configuration of the electric field E_z at each time step.

electric field is not yet visible. At $t = 3T/4$, the concentration of the electric field appears clearly on both the input side and the output side of the gap. The direction of the electric field is different on both sides. At $t = 4T/4$, $5T/4$, $6T/4$, $7T/4$, and $8T/4$, the sinusoidal changing of the field in time continues and the distinct peak of the incident field at the gap appears clearly. Also, the direction of the electric field at both sides of the gap is always in opposition. At the final time step, the field pattern almost shows the steady-state situation. It can also be seen that an x-component of the electric field is excited by the edge effect on the side of the strip.

Fig. 4(b) shows the transient response of the electric field E_x in the *klmn* plane defined by Fig. 4(a). In Fig. 4(b), the time variation of E_x corresponds to the time variation of E_y of the wave in Fig. 3(b). The y-component of the field also occurs because of the edge effect. The concentration of the electric field E_x at the bottom edge of the conductor is larger than on the upper edge. This shows that almost all the lines of electric force grow between the stripline and the ground plane.

Figs. 5(b) and 6(b) show the transient response of the electric field E_z in the *klmn* planes defined by Figs. 5(a) and 6(a), respectively. In these planes, the field is symmetrical about the $y-z$ plane, so only half of the field configuration is shown. Figs. 5(b) and 6(b) present the variations of E_z in time. At $t = T/4$, the wave has not yet reached the gap. At $t = 2T/4$, the amplitude of the wave rises at the input side of the gap, but does not yet appear at the output side of the gap. It can be seen that the 2-component of the electric field has the same sign on both sides of the gap, so the field is almost static in the gap space because the gap is narrow compared with the wavelength. But these figures show that the field strength is larger on the input side of the gap than on the output side. The excitation of the z- and x-components of the field is caused by the edge effect. The concentration of the electric field E_z is largest at the bottom edge

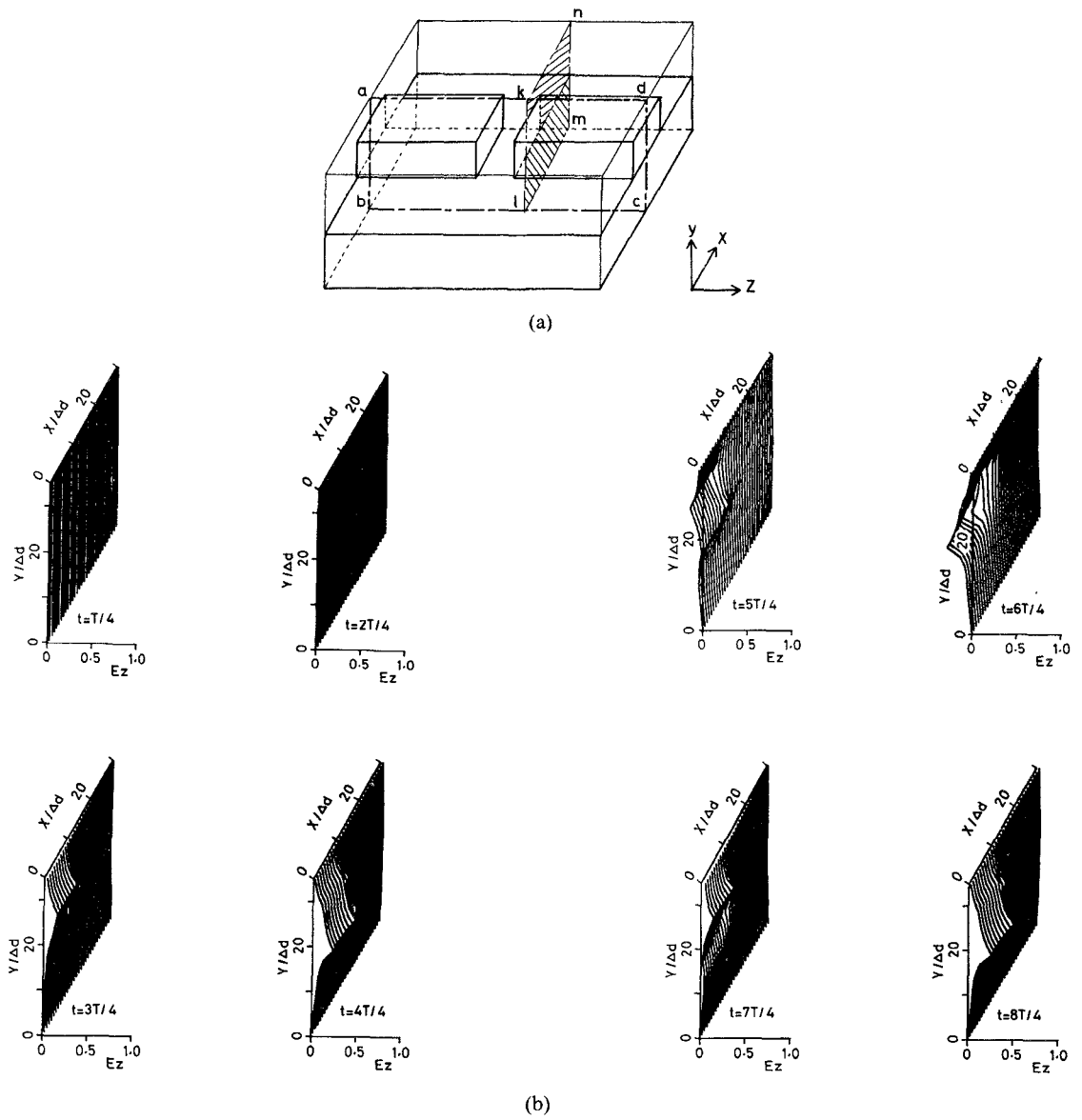

Fig. 6. Transient response of the electric field E_z in the output side plane of the gap. (a) Observation plane of the electric field E_z. (b) Configuration of the electric field E_z at each time step

of the conductor. This shows that lines of electric force emanating from the input side of the gap do not all reach the output side of the gap but rather end up on the ground plane.

IV. Conclusion

The time variation of electromagnetic fields can be described in two ways. Either the instantaneous distribution is shown, as in this paper, or the spatial distribution obtained by taking the envelope of the maximum value during the observation time interval is shown. The former method yields more detailed information on the propagation characteristics of the wave than the latter. We can thus obtain much useful information by studying the transient variation of the amplitude and phase of the fields in the microstrip gap.

In addition, we can easily study the time variations of fields in the case of pulse waves where the analysis of the transient phenomena is very important. The results of the analysis for pulse waves will be reported in a later paper.

References

[1] P. Benedek and P. Silvester, "Equivalent capacitance for microstrip gaps and steps," *IEEE Trans. Microwave Theory Tech.*, vol. MTT-20, pp. 729–733, Nov. 1972.

[2] A. Farrar and A. T. Adams, "Matrix methods for microstrip three-dimensional problems," *IEEE Trans. Microwave Theory Tech*, vol MTT-20, pp. 497–504, Aug. 1972.

[3] S. Koike, N. Yoshida, and I. Fukai, "Transient analysis of microstrip gap," *Trans. IECE Japan*, vol. J67-B, pp 662–669, June 1984.

[4] S. Akhtarzad and P. B. Johns, "Solution of Maxwell's equations in three space dimensions and time by the t.l.m. method of numerical analysis," *Proc. Inst. Elec Eng.*, vol. 122, pp 1344–1348, Dec. 1975.

[5] N. Yoshida and I. Fukai, "Transient analysis of a stripline having a corner in three-dimensional space," *IEEE Trans. Microwave Theory Tech.*, vol. MTT-32, pp. 491–498, May 1984.